

A4-based see-saw model for realistic neutrino masses and mixing

Soumita Pramanick*, Amitava Raychaudhuri†

Department of Physics, University of Calcutta, 92 Acharya Prafulla Chandra Road, Kolkata 700009, India

Abstract

We present an A4-based model where neutrino masses arise from a combination of see-saw mechanisms. The model is motivated by several small mixing and mass parameters indicated by the data. These are θ_{13} , the solar mass splitting, and the small deviation of θ_{23} from maximal mixing ($= \pi/4$). We take the above as indications that at some level the small quantities are well-approximated by zero. In particular the mixing angles, to a zero order, should be either 0 or $\pi/4$. Accordingly, in this model the Type-II see-saw dominates and generates the larger atmospheric mass splitting and sets $\theta_{23} = \pi/4$. The other mixing angles are vanishing as is the solar splitting. We show how the A4 assignment for the lepton doublets leads to this form. We also specify the A4 properties of the right-handed neutrinos which result in a smaller Type-I see-saw contribution that acts as a perturbation and shifts the angles θ_{12} and θ_{13} into the correct range and the desired value of Δm_{solar}^2 is produced. The A4 symmetry results in relationships between these quantities as well as with a small deviation of θ_{23} from $\pi/4$. If the right-handed neutrino mass matrix, M_R , is chosen real then there is no leptonic CP-violation and only Normal Ordering is admissible. If M_R is complex then Inverted Ordering is also allowed with the proviso that the CP-phase, δ , is large, i.e., $\sim \pi/2$ or $-\pi/2$. The preliminary results from NO ν A favouring Normal Ordering and δ near $-\pi/2$ imply quasi-degenerate neutrino masses in this model.

PACS No: 14.60.Pq

Key Words: Neutrino mixing, θ_{13} , Solar splitting, A4, see-saw

I Introduction

Many neutrino oscillation experiments have established that neutrinos are massive and non-degenerate and that the flavour eigenstates are not identical with the mass eigenstates. For the three neutrino paradigm the two independent mass square splittings are the solar (Δm_{solar}^2) and the atmospheric (Δm_{atmos}^2). The mass and flavour bases are related through the Pontecorvo, Maki, Nakagawa, Sakata – PMNS – matrix usually parametrized as:

$$U = \begin{pmatrix} c_{12}c_{13} & s_{12}c_{13} & s_{13}e^{-i\delta} \\ -c_{23}s_{12} + s_{23}s_{13}c_{12}e^{i\delta} & c_{23}c_{12} + s_{23}s_{13}s_{12}e^{i\delta} & -s_{23}c_{13} \\ -s_{23}s_{12} - c_{23}s_{13}c_{12}e^{i\delta} & s_{23}c_{12} - c_{23}s_{13}s_{12}e^{i\delta} & c_{23}c_{13} \end{pmatrix}, \quad (1)$$

where $c_{ij} = \cos \theta_{ij}$ and $s_{ij} = \sin \theta_{ij}$.

The recent measurement of a non-zero value for θ_{13} [1], which is small compared to the other mixing angles, has led to a flurry of activity in developing neutrino mass models which incorporate this feature. Earlier we had demonstrated [2] that a direction which bears exploration is whether two small quantities

*email: soumitapramanick5@gmail.com

†email: palitprof@gmail.com

in the neutrino sector, namely, θ_{13} and the ratio, $R \equiv \Delta m_{solar}^2 / \Delta m_{atmos}^2$, could in fact be related to each other, both resulting from a small perturbation. Subsequently we had shown [3] that it is possible to envisage scenarios where only the larger Δm_{atmos}^2 and $\theta_{23} = \pi/4$ are present in a basic structure of neutrino mass and mixing and the rest of the quantities, namely, θ_{13}, θ_{12} , the deviation of θ_{23} from $\pi/4$, and Δm_{solar}^2 all have their origin in a smaller see-saw induced perturbation¹. Obviously, this gets reflected in constraints on the measured quantities. A vanishing θ_{13} follows rather easily from certain symmetries and indeed many of the newer models are based on perturbations of such structures [5, 6].

Encouraged by the success of this program we present here a model based on the group A_4 which relies on the see-saw mechanism [7] in which the lightest neutrino mass, m_0 , the see-saw scale and one other parameter determine θ_{13} , R , θ_{12} , and the deviation of θ_{23} from $\pi/4$. If this last parameter is complex then the CP-phase δ is also a prediction. Here, the atmospheric mass splitting is taken as an input which together with the lightest neutrino mass completely defines the unperturbed mass matrix generated by the Type-II see-saw. The size of the perturbation is determined by the Type-I see-saw and is of the form m_D^2/m_R where m_D and m_R respectively are the scale of the Dirac and right-handed Majorana mass terms.

After a brief summary of the A_4 group properties and the structure of the model in the following section we describe the implications of the model in the next section. The comparison of this model with the experimental data appears next. We end with our conclusions. The model has a rich scalar field content. In an Appendix we discuss the A_4 invariant scalar potential and the conditions under which the desired potential minimum can be realized.

It should be noted that neutrino mass models based on A_4 have also been investigated earlier [8, 9, 10]. In a majority of them the neutrino mass matrix is obtained from a Type-II see-saw and the earlier emphasis was on obtaining tribimaximal mixing. Recent work has focussed on obtaining more realistic mixing patterns [11] sometimes taking recourse to breaking of A_4 symmetry [12]. Our work is unique in two respects. Firstly, it uses a combination of Type-II and Type-I see-saw mechanisms where the former yields mixing angles which are either vanishing (θ_{12} and θ_{13}) or maximal – i.e., $\pi/4 - (\theta_{23})$ while keeping the solar splitting absent. This kind of a scenario has not been considered before. The Type-I see-saw acting as a perturbation results in a non-zero CP-phase and realistic mixing angles while at the same time creating the correct solar splitting. Secondly, all this is accomplished keeping the A_4 symmetry intact.

II The Model

A_4 is the group of even permutations of four objects comprising of 12 elements which can be generated using the two basic permutations S and T satisfying $S^2 = T^3 = (ST)^3 = \mathbb{I}$. The group has four inequivalent irreducible representations one of 3 dimension and three of 1 dimension denoted by $1, 1'$ and $1''$. The one-dimensional representations are all singlets under S and transform as $1, \omega$, and ω^2 under T respectively, where ω is the cube root of unity. Thus $1' \times 1'' = 1$.

¹Early work on neutrino mass models where some variables are much smaller than others can be found in [4].

Fields	Notations	$A4$	$SU(2)_L$ (Y)	L
Left-handed leptons	$(\nu_i, l_i)_L$	3	2 (-1)	1
Right-handed charged leptons	l_{1R}	1	1 (-2)	1
	l_{2R}	$1'$		
	l_{3R}	$1''$		
Right-handed neutrinos	N_{iR}	3	1 (0)	-1

Table 1: *The fermion content of the model. The transformation properties under $A4$ and $SU(2)_L$ are shown. The hypercharge of the fields, Y , and their lepton number, L , are also indicated.*

For the three-dimensional representation

$$S = \begin{pmatrix} 1 & 0 & 0 \\ 0 & -1 & 0 \\ 0 & 0 & -1 \end{pmatrix} \quad \text{and} \quad T = \begin{pmatrix} 0 & 1 & 0 \\ 0 & 0 & 1 \\ 1 & 0 & 0 \end{pmatrix} . \quad (2)$$

This representation satisfies the product rule

$$3 \otimes 3 = 1 \oplus 1' \oplus 1'' \oplus 3 \oplus 3 . \quad (3)$$

The two triplets arising from the product of $3_a \equiv a_i$ and $3_b \equiv b_i$, where $i = 1, 2, 3$, can be identified as $3_c \equiv c_i$ and $3_d \equiv d_i$ with

$$\begin{aligned} c_i &= \left(\frac{a_2 b_3 + a_3 b_2}{2}, \frac{a_3 b_1 + a_1 b_3}{2}, \frac{a_1 b_2 + a_2 b_1}{2} \right) , \quad \text{or, } c_i \equiv \alpha_{ijk} a_j b_k , \\ d_i &= \left(\frac{a_2 b_3 - a_3 b_2}{2}, \frac{a_3 b_1 - a_1 b_3}{2}, \frac{a_1 b_2 - a_2 b_1}{2} \right) , \quad \text{or, } d_i \equiv \beta_{ijk} a_j b_k , \quad (i, j, k, \text{ are cyclic}) . \end{aligned} \quad (4)$$

In this notation the one-dimensional representations in the $3 \otimes 3$ product can be written as:

$$\begin{aligned} 1 &= a_1 b_1 + a_2 b_2 + a_3 b_3 \equiv \rho_{1ij} a_i b_j , \\ 1' &= a_1 b_1 + \omega^2 a_2 b_2 + \omega a_3 b_3 \equiv \rho_{3ij} a_i b_j , \\ 1'' &= a_1 b_1 + \omega a_2 b_2 + \omega^2 a_3 b_3 \equiv \rho_{2ij} a_i b_j . \end{aligned} \quad (5)$$

Further details of the group $A4$ are available in the literature [8, 9].

In the proposed model the left-handed lepton doublets of the three flavours are assumed to form an $A4$ triplet while the right-handed charged leptons are taken as $1(e_R)$, $1'(\mu_R)$, and $1''(\tau_R)$ under $A4$. The remaining leptons, the right-handed neutrinos, form an $A4$ triplet². The lepton content of the model

²We closely follow the notation of [8].

Purpose	Notations	$A4$	$SU(2)_L$ (Y)	L	vev
Charged fermion mass	$\Phi = \begin{pmatrix} \phi_1^+ & \phi_1^0 \\ \phi_2^+ & \phi_2^0 \\ \phi_3^+ & \phi_3^0 \end{pmatrix}$	3	2 (1)	0	$\langle \Phi \rangle = \frac{v}{\sqrt{3}} \begin{pmatrix} 0 & 1 \\ 0 & 1 \\ 0 & 1 \end{pmatrix}$
Neutrino Dirac mass	$\eta = (\eta^0, \eta^-)$	1	2 (-1)	2	$\langle \eta \rangle = (0, u)$
Type-I see-saw mass	$\hat{\Delta}^L = \begin{pmatrix} \hat{\Delta}_1^{++} & \hat{\Delta}_1^+ & \hat{\Delta}_1^0 \\ \hat{\Delta}_2^{++} & \hat{\Delta}_2^+ & \hat{\Delta}_2^0 \\ \hat{\Delta}_3^{++} & \hat{\Delta}_3^+ & \hat{\Delta}_3^0 \end{pmatrix}^L$	3	3 (2)	-2	$\langle \hat{\Delta}^L \rangle = v_L \begin{pmatrix} 0 & 0 & 1 \\ 0 & 0 & 0 \\ 0 & 0 & 0 \end{pmatrix}$
Type-I see-saw mass	$\Delta_\zeta^L = (\Delta_\zeta^{++}, \Delta_\zeta^+, \Delta_\zeta^0)^L$	1	3 (2)	-2	$\langle \Delta_1^L \rangle = (0, 0, u_L)$
		1'	3 (2)	-2	$\langle \Delta_2^L \rangle = (0, 0, u_L)$
		1''	3 (2)	-2	$\langle \Delta_3^L \rangle = (0, 0, u_L)$
Right-handed neutrino mass	$\hat{\Delta}^R = \begin{pmatrix} \hat{\Delta}_1^0 \\ \hat{\Delta}_2^0 \\ \hat{\Delta}_3^0 \end{pmatrix}^R$	3	1 (0)	2	$\langle \hat{\Delta}^R \rangle = v_R \begin{pmatrix} 1 \\ \omega^2 \\ \omega \end{pmatrix}$
Right-handed neutrino mass	$\Delta_3^R = (\Delta_3^0)^R$	1''	1 (0)	2	$\langle \Delta_3^R \rangle = u_R$

Table 2: *The scalar content of the model. The transformation properties under $A4$ and $SU(2)_L$ are shown. The hypercharge of the fields, Y , their lepton number, L , and the vacuum expectation values are also indicated.*

with the $A4$ and $SU(2)_L$ properties as well as the lepton number assignments is shown in Table 1. Note that the right-handed neutrinos are assigned lepton number -1. This choice is made to ensure that the neutrino Dirac mass matrix takes a form proportional to the identity matrix, as we remark in the following. The assignment of $A4$ quantum numbers of the leptons is by no means unique. The entire list of options for this have been catalogued in [13]. Our choice corresponds to class B of [13]. We do not discuss the extension of this model to the quark sector³.

All lepton masses arise from $A4$ -invariant Yukawa-type couplings. This requires several scalar fields⁴ which develop appropriate vacuum expectation values (vev). To generate the charged lepton masses one uses an $SU(2)_L$ doublet $A4$ triplet of scalar fields Φ_i ($i = 1, 2, 3$). The Type-II see-saw for left-

³For $A4$ -based models dealing with the quark sector see, for example, [14] and [15].

⁴Alternate $A4$ models address this issue by separating the $SU(2)_L$ and $A4$ breakings [9]. The former proceeds through the conventional doublet and triplet scalars which do not transform under $A4$. The $A4$ breaking is triggered through the vev of $SU(2)_L$ singlet ‘flavon’ scalars which transform non-trivially under $A4$. While economy is indeed a virtue here, one pays a price in the form of the effective dimension-5 interactions which have to be introduced to couple the fermion fields simultaneously to the two types of scalars.

handed neutrino masses requires $SU(2)_L$ triplet scalars. The product rule in eq. (3) indicates that these could be in the triplet ($\hat{\Delta}_i^L$), or the singlet 1, 1', 1'' (Δ_ζ^L , $\zeta = 1, 2, 3$) representations of A_4 . As discussed in the following, *all* of these are required to obtain the dominant Type-II see-saw neutrino mass matrix of the form of our choice. The Type-I see-saw results in a smaller contribution whose effect is included perturbatively. For the Dirac mass matrix of the neutrinos an A_4 singlet $SU(2)_L$ doublet η , with lepton number -1, is introduced⁵. The right-handed neutrino mass matrix also arises from Yukawa couplings which respect A_4 symmetry⁶. The scalar fields required for this are all $SU(2)_L$ singlets and under A_4 they transform as triplet ($\hat{\Delta}_i^R$) or the singlet 1'' (Δ_3^R). The scalar fields of the model, their transformation properties under the A_4 and $SU(2)_L$ groups, their lepton numbers and vacuum expectation values are summarized in Table 2.

The Type-I and Type-II mass terms for the neutrinos as well as the charged lepton mass matrix arise from the A_4 and $SU(2)_L$ conserving Lagrangian⁷:

$$\begin{aligned} \mathcal{L}_{mass} &= y_j \rho_{jik} \bar{l}_{Li} l_{Rj} \Phi_k^0 \quad (\text{charged lepton mass}) \\ &+ f \rho_{1ik} \bar{\nu}_{Li} N_{Rk} \eta^0 \quad (\text{neutrino Dirac mass}) \\ &+ \frac{1}{2} (\hat{Y}^L \alpha_{ijk} \nu_{Li}^T C^{-1} \nu_{Lj} \hat{\Delta}_k^{L0} + Y_\zeta^L \rho_{\zeta ij} \nu_{Li}^T C^{-1} \nu_{Lj} \Delta_\zeta^{L0}) \quad (\text{neutrino Type-II see-saw mass}) \\ &+ \frac{1}{2} (\hat{Y}^R \alpha_{ijk} N_{Ri}^T C^{-1} N_{Rj} \hat{\Delta}_k^{R0} + Y_3^R \rho_{3ij} N_{Ri}^T C^{-1} N_{Rj} \Delta_3^{R0}) \quad (\text{rh neutrino mass}) + h.c. \end{aligned} \quad (6)$$

The scalar fields in the above Lagrangian get the following *vevs* (suppressing the $SU(2)_L$ part):

$$\langle \Phi^0 \rangle = \frac{v}{\sqrt{3}} \begin{pmatrix} 1 \\ 1 \\ 1 \end{pmatrix}, \quad \langle \hat{\Delta}^{L0} \rangle = v_L \begin{pmatrix} 1 \\ 0 \\ 0 \end{pmatrix}, \quad \langle \Delta_1^{L0} \rangle = \langle \Delta_2^{L0} \rangle = \langle \Delta_3^{L0} \rangle = u_L, \quad (7)$$

$$\langle \eta^0 \rangle = u, \quad \langle \hat{\Delta}^{R0} \rangle = v_R \begin{pmatrix} 1 \\ \omega^2 \\ \omega \end{pmatrix}, \quad \langle \Delta_3^{R0} \rangle = u_R. \quad (8)$$

The scalar potential involving the fields listed in Table 2 has many terms and is given in an Appendix. There we indicate the conditions under which the scalars achieve the *vev* listed in eqs. (7) and (8).

This results in the charged lepton mass matrix and the left-handed neutrino Majorana mass matrix of the following forms:

$$M_{e\mu\tau} = \frac{v}{\sqrt{3}} \begin{pmatrix} y_1 & y_2 & y_3 \\ y_1 & \omega y_2 & \omega^2 y_3 \\ y_1 & \omega^2 y_2 & \omega y_3 \end{pmatrix}, \quad M_{\nu L} = \begin{pmatrix} (Y_1^L + 2Y_2^L)u_L & 0 & 0 \\ 0 & (Y_1^L - Y_2^L)u_L & \hat{Y}^L v_L / 2 \\ 0 & \hat{Y}^L v_L / 2 & (Y_1^L - Y_2^L)u_L \end{pmatrix}. \quad (9)$$

where we have chosen $Y_2^L = Y_3^L$. In the above the Yukawa couplings satisfy $y_1 v = m_e$, $y_2 v = m_\mu$, $y_3 v = m_\tau$. The Type-II see-saw generates, $M_{\nu L}$, the dominant contribution to the neutrino mass matrix. In the absence of the solar splitting this involves just two masses $m_1^{(0)}$ and $m_3^{(0)}$. To obtain the requisite

⁵ The assignment of opposite lepton numbers to ν_L and N_R forbids their Yukawa coupling with Φ and the Dirac mass matrix can be kept proportional to the identity.

⁶ Since the right-handed neutrinos are $SU(2)_L$ singlets, in principle, one can include direct Majorana mass terms for them. These dimension three terms would break A_4 softly.

⁷ Note that the Dirac mass terms are also L conserving.

structure one must identify $3Y_1^L u_L = 2[2m_1^{(0)} - m_3^{(0)}]$, $3Y_2^L u_L = m_1^{(0)} + m_3^{(0)}$, and $\hat{Y}^L v_L = 2[m_1^{(0)} + m_3^{(0)}]$. The neutrino Dirac mass matrix and the mass matrix of the right-handed neutrinos are:

$$M_D = fu \mathbb{I} \ , \ M_{\nu R} = \begin{pmatrix} Y_3^R u_R & \hat{Y}^R v_R \omega / 2 & \hat{Y}^R v_R \omega^2 / 2 \\ \hat{Y}^R v_R \omega / 2 & Y_3^R u_R \omega^2 & \hat{Y}^R v_R / 2 \\ \hat{Y}^R v_R \omega^2 / 2 & \hat{Y}^R v_R / 2 & Y_3^R u_R \omega \end{pmatrix} . \quad (10)$$

The two unknown combinations appearing in M_R above are expressed as $Y_3^R u_R \equiv (2a + b)$ and $\hat{Y}^R v_R \equiv 2(b - a)$.

The mass matrices in Eq. (9) can be put in a more tractable form by using two transformations, the first being U_L on the left-handed fermion doublets and the other V_R on the right-handed neutrino singlets. U_L and V_R are given by

$$U_L = \frac{1}{\sqrt{3}} \begin{pmatrix} 1 & 1 & 1 \\ 1 & \omega^2 & \omega \\ 1 & \omega & \omega^2 \end{pmatrix} = V_R . \quad (11)$$

No transformation is applied on the right-handed charged leptons. In the new basis, which we call the *flavour* basis, the charged lepton mass matrix is diagonal and the entire lepton mixing resides in the neutrino sector. The mass matrices now are:

$$M_{e\mu\tau}^{flavour} = \begin{pmatrix} m_e & 0 & 0 \\ 0 & m_\mu & 0 \\ 0 & 0 & m_\tau \end{pmatrix} , \ M_{\nu L}^{flavour} = \frac{1}{2} \begin{pmatrix} 2m_1^{(0)} & 0 & 0 \\ 0 & m^+ & -m^- \\ 0 & -m^- & m^+ \end{pmatrix} , \quad (12)$$

and

$$M_D = fu \mathbb{I} \ , \ M_{\nu R}^{flavour} = \frac{1}{2} \begin{pmatrix} 0 & a & 0 \\ a & 0 & 0 \\ 0 & 0 & b \end{pmatrix} . \quad (13)$$

Here $m^\pm = m_3^{(0)} \pm m_1^{(0)}$. m^- is positive for normal ordering (NO) of masses while it is negative for inverted ordering (IO). We use the notation $m_D = fu$.

III Model implications

The A4 model we have presented results in the four mass matrices in eqs. (12) and (13). The lepton mixing and CP-violation will be determined, in this basis, entirely by the neutrino sector on which we focus from here on.

The left-handed neutrino mass matrix $M_{\nu L}^{flavour}$, obtained via a Type-II see-saw, dominates over the Type-I see-saw contribution from the mass matrices in eq. (13). The contribution from the latter is included using perturbation theory.

In the ‘mass basis’ the left-handed neutrino mass matrix is diagonal. The columns of the diagonalising matrix are the unperturbed flavour eigenstates in this basis. We find from $M_{\nu L}^{flavour}$:

$$M^0 = M_{\nu L}^{mass} = U^{0T} M_{\nu L}^{flavour} U^0 = \begin{pmatrix} m_1^{(0)} & 0 & 0 \\ 0 & m_1^{(0)} & 0 \\ 0 & 0 & m_3^{(0)} \end{pmatrix} , \quad (14)$$

the orthogonal matrix, U^0 , being

$$U^0 = \begin{pmatrix} 1 & 0 & 0 \\ 0 & \frac{1}{\sqrt{2}} & -\frac{1}{\sqrt{2}} \\ 0 & \frac{1}{\sqrt{2}} & \frac{1}{\sqrt{2}} \end{pmatrix}. \quad (15)$$

From eqs. (14), (1) and (15) it is seen that the solar splitting is absent, $\theta_{12} = 0$, $\theta_{13} = 0$, $\delta = 0$, and $\theta_{23} = \pi/4$.

Before proceeding with the analysis we would like to remark on the right-handed neutrino Majorana mass matrix in eq. (13), $M_{\nu R}^{flavour}$, which follows from the A_4 symmetric Lagrangian. It has a four-zero texture. This has the virtue of being of a form of $M_{\nu R}^{flavour}$ with the most number of texture zeros. For the see-saw to be operative, the matrix has to be invertible. This eliminates matrices with five texture zeros in the flavour basis. Of the 15 possibilities with four texture zeros there are only two which are invertible and also meet the requirements of the model (i.e., result in a non-zero θ_{12} , θ_{13} , and shift θ_{23} from $\pi/4$). These are:

$$M_1 = \frac{1}{2} \begin{pmatrix} 0 & a & 0 \\ a & 0 & 0 \\ 0 & 0 & b \end{pmatrix}, \quad M_2 = \frac{1}{2} \begin{pmatrix} 0 & 0 & a \\ 0 & b & 0 \\ a & 0 & 0 \end{pmatrix}. \quad (16)$$

Note, $M_1 \leftrightarrow M_2$ under $2 \leftrightarrow 3$ exchange⁸. The results from these two alternatives are very similar except for a few relative signs in the interrelationships among θ_{13} , θ_{12} , and θ_{23} . The $M_{\nu R}^{flavour}$ in eq. (13) is of the form of M_1 . We remark in the end about the changes which entail if the M_2 alternative is used.

Taking a and b as complex we express $M_{\nu R}^{flavour}$ as:

$$M_{\nu R}^{flavour} = m_R \begin{pmatrix} 0 & xe^{-i\phi_1} & 0 \\ xe^{-i\phi_1} & 0 & 0 \\ 0 & 0 & ye^{-i\phi_2} \end{pmatrix}, \quad (17)$$

where x, y are dimensionless real constants of $\mathcal{O}(1)$ and m_R sets the mass-scale. No generality is lost by keeping the Dirac mass real.

In the flavour basis, the Type-I see-saw contribution, which we treat as a perturbation, is:

$$M'^{flavour} = \left[M_D^T (M_{\nu R}^{flavour})^{-1} M_D \right] = \frac{m_D^2}{xym_R} \begin{pmatrix} 0 & ye^{i\phi_1} & 0 \\ ye^{i\phi_1} & 0 & 0 \\ 0 & 0 & xe^{i\phi_2} \end{pmatrix}. \quad (18)$$

In the mass basis it is:

$$M'^{mass} = U^{0T} M'^{flavour} U^0 = \frac{m_D^2}{\sqrt{2} xym_R} \begin{pmatrix} 0 & ye^{i\phi_1} & -ye^{i\phi_1} \\ ye^{i\phi_1} & \frac{xe^{i\phi_2}}{\sqrt{2}} & \frac{xe^{i\phi_2}}{\sqrt{2}} \\ -ye^{i\phi_1} & \frac{xe^{i\phi_2}}{\sqrt{2}} & \frac{xe^{i\phi_2}}{\sqrt{2}} \end{pmatrix}. \quad (19)$$

⁸In the Lagrangian in eq. (6) the replacement $\Delta_3^R \rightarrow \Delta_2^R$, where Δ_2^R transforms like a $1'$ under A_4 , yields an $M_{\nu R}^{flavour}$ of the form of M_2 .

IV Results

After having presented the group-theoretic underpinnings of the model we now indicate its predictions which could be tested in the near future. As noted, from eq. (15) one has $\theta_{23} = \pi/4$ and the other mixing angles are vanishing. Further, once a choice of m_0 , the lightest neutrino mass, is made, depending on the mass ordering either $m_1^{(0)}$ or $m_3^{(0)}$ is determined. The remaining one of these two is fixed so that the atmospheric mass splitting is correctly reproduced. The solar mass splitting, θ_{12} , θ_{13} and the deviation of θ_{23} from maximality are all realized through the first order perturbation, which results in inter-relationships between them. These offer a scope of subjecting the model to experimental probing. From eq. (14) it is seen that to obtain the solar mixing parameters one must take recourse to degenerate perturbation theory.

IV.1 Data

From global fits the currently favoured 3σ ranges of the neutrino mixing parameters are [16, 17]

$$\begin{aligned}\Delta m_{21}^2 &= (7.03 - 8.09) \times 10^{-5} \text{ eV}^2, \quad \theta_{12} = (31.30 - 35.90)^\circ, \\ |\Delta m_{31}^2| &= (2.325 - 2.599) \times 10^{-3} \text{ eV}^2, \quad \theta_{23} = (38.4 - 53.3)^\circ, \\ \theta_{13} &= (7.87 - 9.11)^\circ, \quad \delta = (0 - 360)^\circ.\end{aligned}\tag{20}$$

Here, $\Delta m_{ij}^2 = m_i^2 - m_j^2$, so that $\Delta m_{31}^2 > 0$ (< 0) for normal (inverted) ordering. The data indicate two best-fit points for θ_{23} in the first and second octants. Later, we also use the recent preliminary T2K hints [18] of δ being near $-\pi/2$.

IV.2 Real M_R ($\phi_1 = 0$ or π , $\phi_2 = 0$ or π)

M_R is real if the phases $\phi_{1,2}$ in eq. (17) are 0 or π . For notational simplicity, instead of retaining these phases we allow x (y) to be of either sign, thus capturing the possibilities of ϕ_1 (ϕ_2) being 0 or π .

In the real limit eq. (19) becomes

$$M^{mass} = \frac{m_D^2}{\sqrt{2} x y m_R} \begin{pmatrix} 0 & y & -y \\ y & \frac{x}{\sqrt{2}} & \frac{x}{\sqrt{2}} \\ -y & \frac{x}{\sqrt{2}} & \frac{x}{\sqrt{2}} \end{pmatrix}.\tag{21}$$

The effect of this perturbation on the degenerate solar sector is obtained from the following 2×2 submatrix of the above,

$$M_{2 \times 2}^{mass} = \frac{m_D^2}{\sqrt{2} x y m_R} \begin{pmatrix} 0 & y \\ y & x/\sqrt{2} \end{pmatrix}.\tag{22}$$

This yields

$$\tan 2\theta_{12} = 2\sqrt{2} \left(\frac{y}{x} \right).\tag{23}$$

If $y/x = 1$, i.e., $\hat{Y}^R = 0$ in eq. (10), θ_{12} assumes the tribimaximal value, which though consistent at 3σ is disallowed by the data at 1σ . From the data, $\tan 2\theta_{12} > 0$ always, implying x and y have to be

either both positive or both negative. In other words, $\phi_1 = \phi_2$ and can be either 0 or π . The fitted range of θ_{12} translates to

$$0.682 < \frac{y}{x} < 1.075 \text{ at } 3\sigma . \quad (24)$$

Eqn. (22) also implies

$$\Delta m_{solar}^2 = \frac{m_D^2}{xym_R} m_1^{(0)} \sqrt{x^2 + 8y^2} . \quad (25)$$

Including the first-order corrections from eq. (21) the wave function for the non-degenerate state, $|\psi_3\rangle$, becomes:

$$|\psi_3\rangle = \begin{pmatrix} -\kappa \\ -\frac{1}{\sqrt{2}}(1 - \frac{\kappa}{\sqrt{2}}\frac{x}{y}) \\ \frac{1}{\sqrt{2}}(1 + \frac{\kappa}{\sqrt{2}}\frac{x}{y}) \end{pmatrix} , \quad (26)$$

with

$$\kappa \equiv \frac{m_D^2}{\sqrt{2} x m_R m^-} . \quad (27)$$

For $x > 0$ the sign of κ is the same as that of m^- . Comparing with the third column of eq. (1) one then has

$$\sin \theta_{13} \cos \delta = -\kappa = -\frac{m_D^2}{\sqrt{2} x m_R m^-} . \quad (28)$$

In the case of normal ordering $x > 0$ implies $\delta = \pi$ while for inverted ordering $\delta = 0$, CP remaining conserved in both cases⁹. If $x < 0$ NO (IO) gives $\delta = 0$ (π). From eqs. (28), (23), and (25) one can write,

$$\Delta m_{solar}^2 = -\text{sgn}(x) m^- m_1^{(0)} \frac{4 \sin \theta_{13} \cos \delta}{\sin 2\theta_{12}} , \quad (29)$$

which relates¹⁰ the solar sector with θ_{13} . Once the neutrino mass splittings, and the angles θ_{12} , and θ_{13} are given, eq. (29) fixes the lightest neutrino mass, m_0 .

It can be checked that eq. (29) does not permit inverted ordering. To this end, one defines $z \equiv m^- m_1^{(0)} / \Delta m_{atmos}^2$ and $\tan \xi \equiv m_0 / \sqrt{|\Delta m_{atmos}^2|}$. Note that z is positive for both mass orderings and one has:

$$\begin{aligned} z &= \sin \xi / (1 + \sin \xi) \text{ (normal ordering),} \\ z &= 1 / (1 + \sin \xi) \text{ (inverted ordering) .} \end{aligned} \quad (30)$$

This implies $0 \leq z \leq 1/2$ for NO while $1/2 \leq z \leq 1$ for IO. In both cases z approaches $1/2$ as $m_0 \rightarrow$ large, i.e., one tends towards quasi-degeneracy. From eq. (29)

$$z = \left(\frac{\Delta m_{solar}^2}{|\Delta m_{atmos}^2|} \right) \left(\frac{\sin 2\theta_{12}}{4 \sin \theta_{13} |\cos \delta|} \right) . \quad (31)$$

Bearing in mind that for real M_R one has $|\cos \delta| = 1$ and using the measured values of the other oscillation parameters one finds $z \sim 10^{-2}$. This excludes the inverted mass ordering option.

⁹The mixing angles θ_{ij} are kept in the first quadrant and δ ranges from $-\pi$ to π , as is the convention.

¹⁰It is readily seen from eq. (28) that $-\text{sgn}(x)m^- \cos \delta$ is always positive, ensuring $\Delta m_{solar}^2 > 0$.

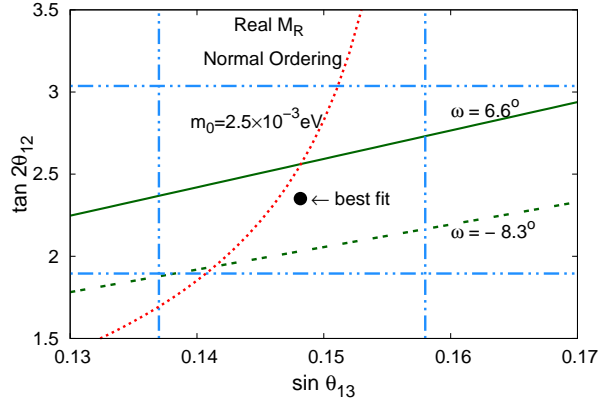


Figure 1: The area inside blue dot-dashed box in the $\sin \theta_{13}$ - $\tan 2\theta_{12}$ plane is allowed by the experimental data at 3σ . The best-fit point is shown as a black dot. The red dotted curve gives the best-fit solar splitting – from eq. (29) – for $m_0 = 2.5$ meV. Using eq. (33) for θ_{23} the area excluded at 3σ is below the green solid (dashed) straight line for the first (second) octant. Only normal ordering is allowed for real M_R .

Further, eq. (26) implies:

$$\tan \theta_{23} \equiv \tan(\pi/4 - \omega) = \frac{1 - \frac{\kappa}{\sqrt{2}} \frac{x}{y}}{1 + \frac{\kappa}{\sqrt{2}} \frac{x}{y}}. \quad (32)$$

Taken together with eqs. (23) and (28) one has

$$\tan \omega = \frac{\kappa}{\sqrt{2}} \frac{x}{y} = -\frac{2 \sin \theta_{13} \cos \delta}{\tan 2\theta_{12}}. \quad (33)$$

When ω is positive (negative), i.e., $\delta = \pi$ (0), we get θ_{23} in the first (second) octant. This corresponds to $x > 0$ ($x < 0$) for NO, the allowed ordering for real M_R .

We are now in a position to state the consequences of this model for real M_R . There are three independent input parameters, namely, m_0 , κ , and y/x which determine θ_{12} , θ_{13} , θ_{23} , and Δm_{solar}^2 for NO. For real M_R inverted ordering is not permitted.

In Fig. 1 the main consequences of this model for real M_R are displayed. The region inside the blue dot-dashed box is the 3σ range of $\sin \theta_{13}$ and $\tan 2\theta_{12}$ from the global fits, the best-fit point being the black dot. From the data in Sec. IV.1 for both octants $\omega_{min} = 0$ at 3σ and $\omega_{max} = 6.6^\circ$ (-8.3°) for the first (second) octant. For the ω_{max} for the first (second) octant eq. (33) of this model corresponds to the green solid (dashed) straight line, the area below being excluded. Further, for real M_R , as $|\cos \delta| = 1$, from eq. (33) we get $|\omega| \geq 5.14^\circ$ for both octants. So far, we have not considered the solar mass splitting. Once Δm_{solar}^2 and $|\Delta m_{atmos}^2|$ are specified, the z (or equivalently m_0) that produces the correct solar splitting for any chosen point in the plane is determined by eq. (31). In this way, using the 3σ ranges of θ_{13} and θ_{12} one finds $z_{max} = 6.03 \times 10^{-2}$, corresponding to $(m_0)_{max} = 3.10$ meV. The consistency of eq. (31) with eq. (33) at ω_{max} sets $z_{min} = 4.01 \times 10^{-2}$ (3.88×10^{-2}) for the first (second) octant which translates to $(m_0)_{min} = 2.13$ (2.06) meV. As an example, choosing $m_0 = 2.5$ meV and taking the best-fit points of the solar and atmospheric mass splittings eq. (29) gives the red dotted curve in Fig. 1.

IV.3 Complex M_R

The shortcomings of the real M_R case – no CP-violation, inverted ordering disallowed – can be overcome when M_R is complex. One then has, as in eq. (19),

$$M'^{mass} = \frac{m_D^2}{\sqrt{2}xym_R} \begin{pmatrix} 0 & ye^{i\phi_1} & -ye^{i\phi_1} \\ ye^{i\phi_1} & \frac{xe^{i\phi_2}}{\sqrt{2}} & \frac{xe^{i\phi_2}}{\sqrt{2}} \\ -ye^{i\phi_1} & \frac{xe^{i\phi_2}}{\sqrt{2}} & \frac{xe^{i\phi_2}}{\sqrt{2}} \end{pmatrix}. \quad (34)$$

x and y are now both positive. Since M' is not hermitian any more the hermitian combination $(M^0 + M')^\dagger(M^0 + M')$ is considered, treating $M^{0\dagger}M^0$ as the unperturbed piece and $(M^{0\dagger}M' + M'^\dagger M^0)$ as the perturbation at lowest order. The zero-order eigenvalues are $(m_i^{(0)})^2$. Written as a 3×3 hermitian matrix the perturbation is

$$(M^{0\dagger}M' + M'^\dagger M^0)^{mass} = \frac{m_D^2}{\sqrt{2}xym_R} \begin{pmatrix} 0 & 2m_1^{(0)}y \cos \phi_1 & -yf(\phi_1) \\ 2m_1^{(0)}y \cos \phi_1 & \frac{2}{\sqrt{2}}m_1^{(0)}x \cos \phi_2 & \frac{1}{\sqrt{2}}xf(\phi_2) \\ -yf^*(\phi_1) & \frac{1}{\sqrt{2}}xf^*(\phi_2) & \frac{2}{\sqrt{2}}m_3^{(0)}x \cos \phi_2 \end{pmatrix}. \quad (35)$$

Above

$$f(\varphi) = m^+ \cos \varphi - im^- \sin \varphi. \quad (36)$$

Eqn. (35) provides the basis for the remaining calculation.

In a manner similar to the real M_R case, from eq. (35) we get

$$\tan 2\theta_{12} = 2\sqrt{2} \frac{y}{x} \frac{\cos \phi_1}{\cos \phi_2}. \quad (37)$$

Since $\tan 2\theta_{12}$ remains positive at 3σ , $\cos \phi_1$ and $\cos \phi_2$ must be of the same sign. The allowed possibilities for these phases are shown in Table 3. We can take over the limits in eq. (24) which now apply on $(y/x)(\cos \phi_1 / \cos \phi_2)$.

In place of eq. (26) we now have at first order:

$$|\psi_3\rangle = \begin{pmatrix} -\kappa f(\phi_1)/m^+ \\ -\frac{1}{\sqrt{2}}[1 - \frac{\kappa}{\sqrt{2}}\frac{x}{y} f(\phi_2)/m^+] \\ \frac{1}{\sqrt{2}}[1 + \frac{\kappa}{\sqrt{2}}\frac{x}{y} f(\phi_2)/m^+] \end{pmatrix}. \quad (38)$$

Since x, y are now positive quantities, the sign of κ is determined by that of m^- , i.e., κ is positive (negative) for normal (inverted) ordering. From eqs. (1) and (38)

$$\begin{aligned} \sin \theta_{13} \cos \delta &= -\kappa \cos \phi_1, \\ \sin \theta_{13} \sin \delta &= -\kappa \frac{m^-}{m^+} \sin \phi_1. \end{aligned} \quad (39)$$

Using eq. (39) one can immediately relate the quadrant of δ with that of ϕ_1 for both orderings. These are also presented in Table 3. It can be seen that a near-maximal $\delta = -\pi/2 - \epsilon$ is obtained for normal (inverted) ordering if $\phi_1 \sim -\pi/2 - \epsilon$ ($-\pi/2 + \epsilon$).

ϕ_1 quadrant	ϕ_2 quadrant	Normal Ordering		Inverted Ordering	
		δ quadrant	θ_{23} octant	δ quadrant	θ_{23} octant
$0 - \pi/2$	$0 - \pi/2$ or $-\pi/2 - 0$	$-\pi - -\pi/2$	$0 - \pi/4$	$-\pi/2 - 0$	$\pi/4 - \pi/2$
$\pi/2 - \pi$	$\pi/2 - \pi$ or $-\pi - -\pi/2$	$-\pi/2 - 0$	$\pi/4 - \pi/2$	$-\pi - -\pi/2$	$0 - \pi/4$
$-\pi - -\pi/2$	$\pi/2 - \pi$ or $-\pi - -\pi/2$	$0 - \pi/2$	$\pi/4 - \pi/2$	$\pi/2 - \pi$	$0 - \pi/4$
$-\pi/2 - 0$	$0 - \pi/2$ or $-\pi/2 - 0$	$\pi/2 - \pi$	$0 - \pi/4$	$0 - \pi/2$	$\pi/4 - \pi/2$

Table 3: *The options for the phase ϕ_1 in M_R and the consequent ranges of the other phase ϕ_2 in M_R , the leptonic CP-phase δ , and the octant of θ_{23} for both mass orderings. All angles are in radians. For inverted ordering or quasi-degeneracy $\delta \sim \pi/2$ or $-\pi/2$.*

In addition, for θ_{23} eq. (38) implies

$$\tan \theta_{23} = \frac{1 - \frac{\kappa_x x}{\sqrt{2} y} \cos \phi_2}{1 + \frac{\kappa_x x}{\sqrt{2} y} \cos \phi_2} . \quad (40)$$

The deviation from maximality, ω , can be obtained from the above and using eqs. (37) and (39) expressed as

$$\tan \omega = -\frac{2 \sin \theta_{13} \cos \delta}{\tan 2\theta_{12}} , \quad (41)$$

which has the same form as eq. (33) for the real M_R case except that now $\cos \delta$ can deviate from ± 1 . The octant of θ_{23} for different choices of ϕ_1 quadrants is given in Table 3 for both mass orderings.

Substituting for m_D^2/m_R in terms of $\sin \theta_{13} \cos \delta$, using eq. (39) one has from eq. (35)

$$\Delta m_{solar}^2 = -\text{sgn}(\cos \phi_2) m^- m_1^{(0)} \frac{4 \sin \theta_{13} \cos \delta}{\sin 2\theta_{12}} , \quad (42)$$

which is reminiscent of eq. (29) for real M_R . Keeping in mind that $\cos \phi_1 / \cos \phi_2$ must be positive and using eq. (39) it is easy to see that $\Delta m_{solar}^2 > 0$ always. Since the sign of ω – i.e., the octant of θ_{23} – depends on the quadrant of only $\cos \phi_1$, irrespective of the mass ordering one can accommodate both octants while meeting the solar splitting requirement.

As in eq. (31) one again has

$$|\cos \delta| = \left(\frac{\Delta m_{solar}^2}{|\Delta m_{atmos}^2|} \right) \left(\frac{\sin 2\theta_{12}}{4 \sin \theta_{13} z} \right) , \quad (43)$$

with the further proviso that $|\cos \delta|$ can now be anywhere between zero and unity. This freedom removes the bar which applied on inverted ordering for real M_R .

Here we use m_0, θ_{13} , and θ_{12} as inputs to fix the model parameters. Eqs. (41) and (43) then determine θ_{23} and δ respectively, as shown in Figs. 2 and 3. One can also obtain $|m_{\nu_e \nu_e}|$, which determines the neutrino-less double-beta decay rate, in terms of the mass eigenvalues and the mixing angles. In these figures the green (pink) curves are for NO (IO).

In the left panel of Fig. 2 the dependence of θ_{23} on m_0 is presented while the right panel shows $|m_{\nu_e \nu_e}|$ again as a function of m_0 . The thick lines delimit the 3σ allowed regions while the thin lines correspond

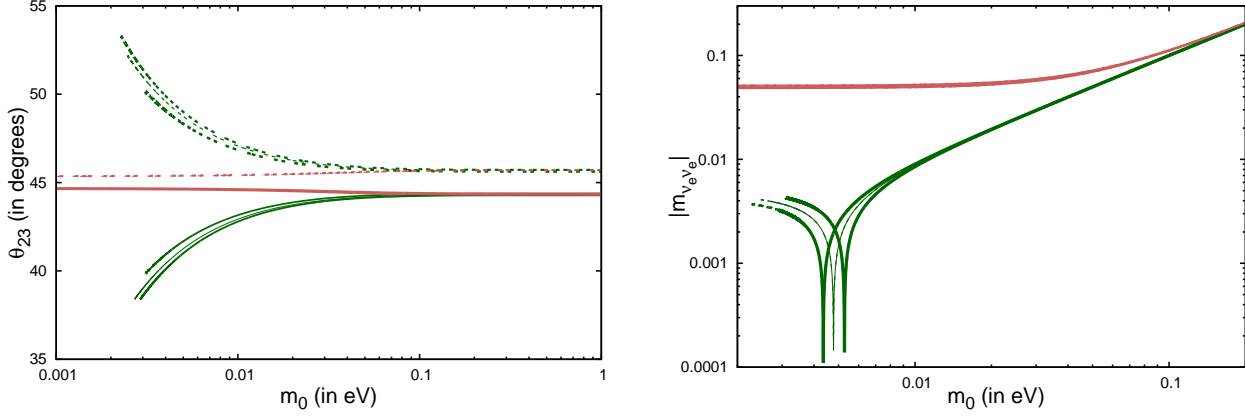


Figure 2: θ_{23} (left panel) and $|m_{\nu_e \nu_e}|$, the quantity controlling neutrino-less double-beta decay, in eV (right panel) as a function of the lightest neutrino mass m_0 (in eV). The green (pink) curves are for NO (IO). The 3σ allowed region is between the thick curves while the thin curves are for the best-fit input values. The solid (dashed) curves are for the first (second) octant of θ_{23} .

to the best-fit values of input parameters. The solid (dashed) curves are for the first (second) octant of θ_{23} . The thick and thin curves for IO overlap and cannot be distinguished. As expected from eq. (41) θ_{23} is symmetric about $\pi/4$. The experimental 3σ bounds on θ_{23} for both octants determine a minimum permitted m_0 for NO. For IO there is no such lower bound. Planned experiments to measure the neutrino mass [19] are sensitive to m_0 not less than 200 meV. From Fig. 2 it is seen that at such a scale the two mass orderings have close predictions, which is a reflection of quasi-degeneracy.

In the left panel of Fig. 3 we show the dependence of δ on m_0 for both NO and IO. The line-type conventions are the same as in Fig. 2. As noted in Table 3 and eq. (39), δ can be in any of the four quadrants depending on the choice of ϕ_1 . Eq. (43) indicates that for all these four cases, namely, $\pm\delta$ and $\pm(\pi - \delta)$, the dependence of $|\cos \delta|$ on m_0 is identical for a chosen mass ordering. Keeping this in mind, Fig. 3 (left panel) has been plotted with δ in the first quadrant. For m_0 smaller than ~ 10 meV, δ differs significantly for the two orderings. As expected from Fig. 1, the real M_R limit, i.e., $\delta = 0$, is obtained only for NO.

The variation of δ with $\sin^2 2\theta_{13}$ obtained from eq. (42) for both mass orderings for two representative values of $m_0 = 0.5$ eV (solid curves) and 2.5 meV (dashed curves) is shown in the right panel of Fig. 3. Here the best-fit values of the two mass splittings and θ_{12} have been used. The allowed range of $\sin^2 2\theta_{13}$ from the global fits at 3σ (1σ) is bounded by the blue solid (dot-dashed) vertical lines. Note that in all cases there are solutions for δ in every quadrant. For IO δ remains close to $\pm\pi/2$ for all m_0 . For NO, with $m_0 = 0.5$ eV, which is in the quasi-degenerate region, δ is the same as for IO while for $m_0 = 2.5$ meV one finds δ around 0 or $\pm\pi$ and that too for a limited range of $\sin^2 2\theta_{13}$. In this panel we have also shown 90% C.L. exclusion limits in the $\sin^2 2\theta_{13} - \delta$ plane – dotted curves – identified by the T2K collaboration. The regions to the left of the curves are disfavoured. Notice that $\delta = -\pi/2$ is preferred, which in our model is consistent with IO for all masses but a limited range of $\sin^2 2\theta_{13}$ while for NO though the full range of the latter is consistent one must have $m_0 \geq 100$ meV. More precise measurements of neutrino parameters will test this model closely.

Finally, it is noteworthy that the phase ϕ_2 enters only in three places: in the combination $x \cos \phi_2 / y$

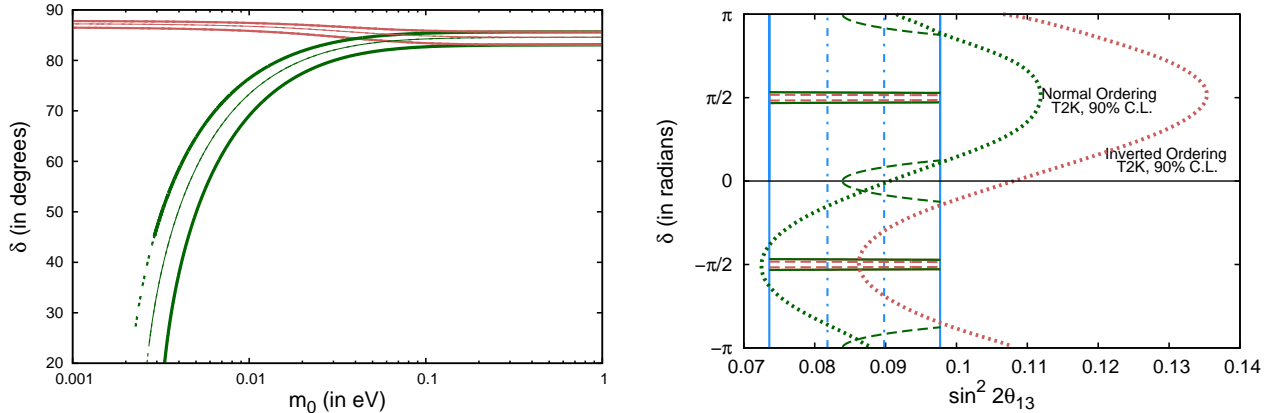


Figure 3: *The CP-phase δ from this model. The green (pink) curves are for NO (IO). Left: δ as a function of m_0 in eV. The line-type conventions are as in Fig. 2. Results are shown only for the first quadrant. Right: The blue vertical solid (dot-dashed) lines are the 3σ (1σ) allowed ranges of $\sin^2 2\theta_{13}$ from global fits. Dependence of δ for $m_0 = 0.5$ eV ($m_0 = 2.5$ meV) on $\sin^2 2\theta_{13}$ within the allowed range are the solid (dashed) lines. The curves for $m_0 = 0.5$ eV for the two orderings overlap. Also shown are the 90% C.L. curves (dotted) obtained by T2K [18] which disallow the region to their left.*

in the expressions for $\tan 2\theta_{12}$ and $\tan \theta_{23}$ - eqs. (37) and (40), and as $\text{sgn}(\cos \phi_2)$ in the formula for the solar splitting - eq. (42). So, its effect can be entirely subsumed by redefining $\cos \phi_2/y \rightarrow 1/y$ and permitting y to be both positive and negative. Therefore for complex M_R the free input parameters are really m_0 , κ , y/x and ϕ_1 which determine the three mixing angles, the solar mass splitting, and the CP-phase δ .

Before concluding, we would like to make a comment on our choice of M_R . In eq. (16) two four-zero textures, M_1 and M_2 , were identified both of which could be admissible for M_R . We had chosen M_1 for this work. If instead, we had chosen M_2 then the discussion would go through essentially unchanged except for the replacement $\kappa \rightarrow -\kappa$.

V Conclusions

We have proposed a model for neutrino masses and lepton mixing which relies on an underlying $A4$ symmetry. All masses are generated from $A4$ invariant Yukawa couplings. There are contributions to the neutrino masses from both Type-I and Type-II see-saw terms of which the latter is dominant. It generates the atmospheric mass splitting and keeps the mixing angles either maximal, e.g., $\pi/4$ for θ_{23} , or vanishing, for θ_{13} and θ_{12} . The solar splitting is absent. The Type-I see-saw contribution, which is treated perturbatively, results in θ_{13} , θ_{12} , and θ_{23} consistent with the global fits and generates the solar splitting. Both octants of θ_{23} are permitted. Testable relationships between these quantities, characteristic of this model, are derived. As another example, inverted ordering of neutrino masses is correlated with a near-maximal CP-phase δ and allows arbitrarily small neutrino masses. For normal ordering δ can vary over the entire range and approaches maximality in the quasi-degenerate limit. The lightest neutrino mass cannot be lower than a few meV in this case.

While this paper was being finalised, $\text{NO}\nu\text{A}$ announced [20] their preliminary results based on the equivalent of 2.74×10^{20} p.o.t. With $\sin^2 \theta_{23} = 0.50$ the data favour NO and at 90% CL indicate δ between $-\pi$ to 0 with a preference for $\delta \sim -\pi/2$. As seen from Fig. 3 this is consistent with our model, with $\delta \sim -\pi/2$ favouring m_0 in the quasi-degenerate regime, i.e., $m_0 \geq \mathcal{O}(0.1 \text{ eV})$. If this result is confirmed by further analysis then the model will require neutrino masses to be in a range to which ongoing experiments will be sensitive [21].

Acknowledgements: SP acknowledges support from CSIR, India. AR is partially funded by the Department of Science and Technology Grant No. SR/S2/JCB-14/2009.

Appendix: The scalar potential minimization

In this Appendix we discuss the nature of the scalar potential of the model in some detail. We also identify the conditions which must be satisfied by the parameters of the potential so that the *neutrinos* take the values considered in the model. Needless to say, the conditions ensure that the potential is locally minimized by this choice. To check whether it is also a *global* minimum is beyond the scope of this paper¹¹.

The scalars listed in Table 2 have fields transforming under A_4 , $SU(2)_L$, and $U(1)_Y$ which also carry a lepton number. The scalar potential has to be of the most general quartic form which is a singlet under all these symmetries. Below we include all terms that are permitted by the symmetries. Invariance under $SU(2)_L$, $U(1)_Y$ and lepton number are easy to verify.

A.1 A_4 invariants: Notation and generalities

Here we give a brief account of our notation and the A_4 -invariant terms. First recall that there are scalars which transform as 1, 1', 1'', and 3 under A_4 . One must include in the potential up to quartics in these fields which give rise to A_4 singlets. The product rules of the one-dimensional representations 1, 1' and 1'' are simple, it is the A_4 triplet which requires some discussion. To this end consider two A_4 triplet fields $A \equiv (a_1, a_2, a_3)^T$ and $B \equiv (b_1, b_2, b_3)^T$ where a_i, b_i may have $SU(2)_L \times U(1)_Y$ transformation properties which we suppress here. As noted in eq. (3), combining A and B one can obtain

$$3_A \otimes 3_B = 1 \oplus 1' \oplus 1'' \oplus 3 \oplus 3 \ . \quad (\text{A.1})$$

We denote the irreducible representations on the right-hand-side by $O_1(A, B)$, $O_2(A, B)$, $O_3(A, B)$, $T_s(A, B)$ and $T_a(A, B)$, respectively, where, as noted in eqs. (4, 5)

$$\begin{aligned} O_1(A, B) &\equiv 1 = a_1 b_1 + a_2 b_2 + a_3 b_3 \equiv \rho_{1ij} a_i b_j \ , \\ O_2(A, B) &\equiv 1' = a_1 b_1 + \omega^2 a_2 b_2 + \omega a_3 b_3 \equiv \rho_{3ij} a_i b_j \ , \\ O_3(A, B) &\equiv 1'' = a_1 b_1 + \omega a_2 b_2 + \omega^2 a_3 b_3 \equiv \rho_{2ij} a_i b_j \ , \end{aligned} \quad (\text{A.2})$$

and

$$T_s(A, B) \equiv 3 = \left(\frac{a_2 b_3 + a_3 b_2}{2}, \frac{a_3 b_1 + a_1 b_3}{2}, \frac{a_1 b_2 + a_2 b_1}{2} \right)^T \ ,$$

¹¹For example, the global minima of the relatively simple case of one A_4 triplet $SU(2)_L$ doublet scalar multiplet have been identified in [22] and used in the context of a model for leptons in [23].

$$T_a(A, B) \equiv 3 = \left(\frac{a_2 b_3 - a_3 b_2}{2}, \frac{a_3 b_1 - a_1 b_3}{2}, \frac{a_1 b_2 - a_2 b_1}{2} \right)^T. \quad (\text{A.3})$$

Note that $O_3(A^\dagger, A) = [O_2(A^\dagger, A)]^\dagger$ and $T_a(A, A) = 0$.

The scalar potential can be written in this notation keeping in mind the following:

- No two scalar multiplets have all quantum numbers the same. So terms in the potential cannot be related by replacing any one field by some other.
- Neither is there a scalar which is a singlet under all the symmetries.

Thus the scalar potential can consist of terms of the following forms (displaying only $A4$ behaviour):

1. Quadratic: $W^\dagger W$,
2. Cubic: $X_i X'_j X''_k, X_i X_j X_k, X'_i X'_j X'_k, X''_i X''_j X''_k, O_1(Y_i, Y_j) X_k, O_2(Y_i, Y_j) X''_k, O_3(Y_i, Y_j) X'_k$,
3. Quartic:

$$(W_i^\dagger W_i)(W_j^\dagger W_j), (X_i X_j)(X_k X_l), (X_i X_j)(X'_k X'_l), (X'_i X'_j)(X'_k X'_l), (X'_i X'_j)(X'_k X_l), (X''_i X''_j)(X''_k X_l),$$

$$O_1(Y_i, Y_j) X_k X_l, O_1(Y_i, Y_j) X'_k X'_l, O_2(Y_i, Y_j) X'_k X'_l, O_2(Y_i, Y_j) X_k X''_l,$$

$$O_3(Y_i, Y_j) X'_k X''_l, O_3(Y_i, Y_j) X_k X'_l,$$

$$O_1(Y_i, Y_j) O_1(Y_k, Y_l), O_2(Y_i, Y_j)^\dagger O_2(Y_k, Y_l), O_3(Y_i, Y_j)^\dagger O_3(Y_k, Y_l), O_2(Y_i, Y_j) O_3(Y_k, Y_l),$$

$$O_1(T_s(Y_i, Y_j), T_s(Y_k, Y_l)), O_1(T_s(Y_i, Y_j), T_a(Y_k, Y_l)), O_1(T_a(Y_i, Y_j), T_a(Y_k, Y_l)).$$

$$O_1(T_s(Y_i, Y_j), Y_k) X_l, O_2(T_s(Y_i, Y_j), Y_k) X''_l, O_3(T_s(Y_i, Y_j), Y_k) X'_l,$$

$$O_1(T_a(Y_i, Y_j), Y_k) X_l, O_2(T_a(Y_i, Y_j), Y_k) X''_l, O_3(T_a(Y_i, Y_j), Y_k) X'_l.$$

In the above W is any field, X, X' , and X'' stand for generic fields transforming as 1, $1'$, and $1''$ under $A4$ while Y is a generic $A4$ triplet field. We have not separately listed the invariants formed using $X^\dagger, X'^\dagger, X''^\dagger$, and Y^\dagger .

Because of the large number of scalar fields in our model – e.g., $SU(2)_L$ singlets, doublets, and triplets – the scalar potential has many terms. To simplify this discussion, we exclude cubic terms in the fields and take all couplings in the potential to be real. For ease of presentation, we list the potential in separate pieces: (a) those restricted to any one $SU(2)_L$ sector, and (b) those coupling scalars of different $SU(2)_L$ sectors. Since the *vev* of the $SU(2)_L$ singlets, which are responsible for the right-handed neutrino mass, are much larger than that of the other scalars, in the latter category we keep only the terms which couple the singlet fields to either the doublet or the triplet sectors.

A.2 $SU(2)_L$ Singlet Sector:

In the $SU(2)_L$ singlet scalar sector there is an $A4$ triplet $\hat{\Delta}^R$ and another scalar Δ_3^R that transforms as a $1''$. Eq. (A.1) shows that two $\hat{\Delta}^R$ triplets can combine to give different $A4$ irreducible representations. For this purpose we introduce the notations:

$$O_1^{ss} \equiv O_1(\hat{\Delta}^{R\dagger}, \hat{\Delta}^R); \quad O_2^{ss} \equiv O_2(\hat{\Delta}^{R\dagger}, \hat{\Delta}^R); \quad T_s^{ss} \equiv T_s(\hat{\Delta}^R, \hat{\Delta}^R). \quad (\text{A.4})$$

Generically, we will use the notation \tilde{O}_i or $\tilde{T}_{s,a}$ if the second $A4$ triplet field in the argument is replaced by its hermitian conjugate. For example, here

$$\tilde{O}_3^{ss} \equiv O_3(\hat{\Delta}^{R\dagger}, \hat{\Delta}^{R\dagger}) \text{ and } \tilde{T}_s^{ss} \equiv T_s(\hat{\Delta}^R, \hat{\Delta}^{R\dagger}). \quad (\text{A.5})$$

We will also require the combinations:

$$\mathcal{O}_2^{ss} \equiv O_2(\hat{\Delta}^R, T_s^{ss\dagger}). \quad (\text{A.6})$$

From the $A4$ singlet Δ_3^R one can make the combination

$$Q_3^{ss} \equiv \Delta_3^{R\dagger} \Delta_3^R, \quad (\text{A.7})$$

which is obviously a singlet under all the symmetries.

Using this notation the most general scalar potential of this sector is given by:

$$\begin{aligned} V_{singlet} &= m_{\Delta_3^R}^2 Q_3^{ss} + m_{\hat{\Delta}^R}^2 O_1^{ss} + \frac{1}{2} \lambda_1^s [Q_3^{ss}]^2 + \frac{1}{2} \lambda_2^s \left\{ [O_1^{ss}]^2 + (O_2^{ss})^\dagger O_2^{ss} + O_1(T_s^{ss}, T_s^{ss\dagger}) \right\} \\ &+ \frac{1}{2} \lambda_3^s [Q_3^{ss} O_1^{ss}] + \lambda_4^s [\mathcal{O}_2^{ss} \Delta_3^R + \text{h.c.}] + \lambda_5^s \left[\tilde{O}_3^{ss} \Delta_3^R \Delta_3^R + \text{h.c.} \right]. \end{aligned} \quad (\text{A.8})$$

In the above, we have taken λ_2^s as the common coefficient of the different $A4$ -singlets that can be obtained from the combination of two $\hat{\Delta}^R$ and two $(\hat{\Delta}^R)^\dagger$ fields. We also follow a similar principle for the fields with other $SU(2)_L$ behaviour.

A.3 $SU(2)_L$ Doublet Sector:

The $SU(2)_L$ doublet scalar sector comprises of the two fields Φ and η transforming as 3 and 1 under $A4$ respectively. Recall that Φ and η have opposite hypercharge. In analogy to the singlet sector we denote the required $A4$ triplet Φ combinations as:

$$O_1^{dd} \equiv O_1(\Phi^\dagger, \Phi); \quad O_2^{dd} \equiv O_2(\Phi^\dagger, \Phi); \quad T_s^{dd} \equiv T_s(\Phi, \Phi), \quad (\text{A.9})$$

and from the $A4$ singlet η

$$Q_\eta^{dd} \equiv \eta^\dagger \eta. \quad (\text{A.10})$$

The potential for this sector is:

$$\begin{aligned} V_{doublet} &= m_\eta^2 Q_\eta^{dd} + m_\Phi^2 O_1^{dd} + \frac{1}{2} \lambda_1^d [Q_\eta^{dd}]^2 + \frac{1}{2} \lambda_2^d \left\{ [O_1^{dd}]^2 + \{O_2^{dd}\}^\dagger O_2^{dd} \right. \\ &+ \left. O_1(T_s^{dd}, T_s^{dd\dagger}) \right\} + \frac{1}{2} \lambda_3^d [Q_\eta^{dd} O_1^{dd}]. \end{aligned} \quad (\text{A.11})$$

A.4 $SU(2)_L$ Triplet Sector:

The $SU(2)_L$ triplet sector consists of four fields, viz, $\hat{\Delta}^L$, Δ_1^L , Δ_2^L and Δ_3^L transforming as 3, 1, 1', 1'' under $A4$.

We define

$$O_1^{tt} \equiv O_1(\hat{\Delta}^{L\dagger}, \hat{\Delta}^L); \quad O_2^{tt} \equiv O_2(\hat{\Delta}^{L\dagger}, \hat{\Delta}^L); \quad T_s^{tt} \equiv T_s(\hat{\Delta}^L, \hat{\Delta}^L), \quad (\text{A.12})$$

$$Q_i^{tt} \equiv \Delta_i^{L\dagger} \Delta_i^L, \quad (i = 1, 2, 3), \quad (\text{A.13})$$

and

$$\mathcal{O}_i^{tt} \equiv O_i(\hat{\Delta}^L, T_s^{tt\dagger}) \quad (i = 1, 2, 3). \quad (\text{A.14})$$

The scalar potential for this sector:

$$\begin{aligned} V_{\text{triplet}} &= \sum_{i=1}^3 m_{\Delta_i^L}^2 Q_i^{tt} + m_{\hat{\Delta}^L}^2 O_1^{tt} + \frac{1}{2} \sum_{i=1}^3 \lambda_{1_i}^t [Q_i^{tt}]^2 + \frac{1}{2} \sum_{k<j, k=1}^2 \sum_{j=2}^3 \lambda_{2jk}^t Q_j^{tt} Q_k^{tt} \\ &+ \frac{1}{2} \lambda_3^t \left\{ [O_1^{tt}]^2 + \{O_2^{tt}\}^\dagger O_2^{tt} + O_1(T_s^{tt}, T_s^{tt\dagger}) \right\} + \frac{1}{2} \sum_{i=1}^3 \lambda_{4_i}^t [Q_i^{tt} O_1^{tt}] \\ &+ \lambda_5^t [\mathcal{O}_1^{tt} \Delta_1^L + \text{h.c.}] + \lambda_6^t [\mathcal{O}_3^{tt} \Delta_2^L + \text{h.c.}] + \lambda_7^t [\mathcal{O}_2^{tt} \Delta_3^L + \text{h.c.}] \\ &+ \sum_{i=1}^3 \lambda_{8_i}^t \left[\tilde{O}_i^{tt} \Delta_i^L \Delta_i^L + \text{h.c.} \right] + \left[\lambda_{9_1}^t \tilde{O}_1^{tt} \Delta_2^L \Delta_3^L + \text{h.c.} + \text{cyclic} \right]. \quad (\text{A.15}) \end{aligned}$$

A.5 Inter-sector terms:

So far, we have listed the terms in the potential that involve scalar fields which belong to any one of three sectors: singlets, doublets, or triplets of $SU(2)_L$. Besides these, there will also be terms in the scalar potential which involve fields from multiple sectors. Below we list the terms which arise from couplings of the singlet sector with either the doublet or the triplet sector. The other inter-sector terms – doublet-triplet type – are dropped. Since the vacuum expectation values of the singlet fields are by far the largest this is not an unreasonable approximation.

A.5.1 Inter-sector Singlet-Doublet terms:

It is useful to define,

$$\tilde{T}_s^{ss} \equiv T_s(\hat{\Delta}^R, \hat{\Delta}^{R\dagger}), \quad \text{and} \quad \tilde{T}_s^{dd} \equiv T_s(\Phi, \Phi^\dagger), \quad (\text{A.16})$$

and

$$O_{1S}^{sd} \equiv O_1(\tilde{T}_s^{dd}, \tilde{T}_s^{ss}); \quad \mathcal{O}_3^{sd} \equiv O_3(\hat{\Delta}^R, \tilde{T}_s^{dd}). \quad (\text{A.17})$$

For simplicity, we do not keep the combinations $\tilde{T}_a^{ss} \equiv T_a(\hat{\Delta}^R, \hat{\Delta}^{R\dagger})$ and $\tilde{T}_a^{dd} \equiv T_a(\Phi, \Phi^\dagger)$.

In terms of the above:

$$\begin{aligned} V_{sd} &= \frac{1}{2} \lambda_1^{sd} [Q_3^{ss} Q_\eta^{dd}] + \frac{1}{2} \lambda_2^{sd} [Q_3^{ss} O_1^{dd}] + \frac{1}{2} \lambda_3^{sd} [Q_\eta^{dd} O_1^{ss}] + \lambda_4^{sd} [\{\mathcal{O}_3^{sd}\}^\dagger \Delta_3^R + \text{h.c.}] \\ &+ \frac{1}{2} \lambda_5^{sd} [O_1^{dd} O_1^{ss} + \{O_2^{ss}\}^\dagger O_2^{dd} + \{O_2^{dd}\}^\dagger O_2^{ss} + O_{1S}^{sd}]. \quad (\text{A.18}) \end{aligned}$$

Here, in the last term, we have made the simplifying assumption that there is a common coupling λ_5^{sd} for the terms in the potential which arise from various combinations of $(\Phi^\dagger \Phi)(\hat{\Delta}^{R\dagger} \hat{\Delta}^R)$, each of the four fields being $A4$ triplets.

A.5.2 Inter-sector Singlet-Triplet terms:

For this case the following combinations arise:

$$\begin{aligned} O_i^{ts} &\equiv O_i(\hat{\Delta}^{R\dagger}, \hat{\Delta}^L) \quad (i = 1, 2, 3); O_{1S}^{ts} \equiv O_1(\tilde{T}_s^{tt}, \tilde{T}_s^{ss}); \\ \tilde{O}_i^{ts} &\equiv O_i(\tilde{T}_s^{ss}, \hat{\Delta}^L) \quad (i = 1, 2, 3); \tilde{O}_3^{ts} \equiv O_3(\tilde{T}_s^{tt}, \hat{\Delta}^R) . \end{aligned} \quad (\text{A.19})$$

In line with the convention introduced earlier: $\tilde{O}_i^{ts} \equiv O_i(\hat{\Delta}^{R\dagger}, \hat{\Delta}^{L\dagger}) \quad (i = 1, 2, 3)$.

The intersector potential for this case is given by:

$$\begin{aligned} V_{ts} &= \frac{1}{2} \sum_{i=1}^3 \lambda_i^{ts} [Q_3^{ss} Q_i^{tt}] + \frac{1}{2} \lambda_2^{ts} [Q_3^{ss} O_1^{tt}] + \frac{1}{2} \sum_{i=1}^3 \lambda_{3i}^{ts} [Q_i^{tt} O_1^{ss}] \\ &+ \frac{1}{2} \lambda_4^{ts} [O_1^{tt} O_1^{ss} + \{O_2^{ss}\}^\dagger O_2^{tt} + \{O_2^{tt}\}^\dagger O_2^{ss} + O_{1S}^{ts}] \\ &+ \sum_{i=1}^3 \lambda_{5i}^{ts} [\mathcal{O}_i^{ts} \Delta_i^{L\dagger} + h.c.] + \lambda_6^{ts} [\tilde{\mathcal{O}}_3^{ts} \Delta_3^{R\dagger} + h.c.] \\ &+ \lambda_7^{ts} [O_1^{ts} \Delta_3^{L\dagger} \Delta_3^R + h.c.] + \lambda_8^{ts} [O_2^{ts} \Delta_1^{L\dagger} \Delta_3^R + h.c.] + \lambda_9^{ts} [O_3^{ts} \Delta_2^{L\dagger} \Delta_3^R + h.c.] \\ &+ \lambda_{10}^{ts} [\tilde{O}_3^{ts} \Delta_3^R \Delta_1^L + h.c.] + \lambda_{11}^{ts} [\tilde{O}_2^{ts} \Delta_3^R \Delta_3^L + h.c.] + \lambda_{12}^{ts} [\tilde{O}_1^{ts} \Delta_3^R \Delta_2^L + h.c.] . \end{aligned} \quad (\text{A.20})$$

A.6 The minimization conditions:

After having presented the scalar potential we now seek to find the conditions under which the vev we have used in the model – see eqs. (7) and (8) and Table 2 – constitute a local minimum. For ready reference the vev are:

$$\langle \Phi^0 \rangle = \frac{v}{\sqrt{3}} \begin{pmatrix} 1 \\ 1 \\ 1 \end{pmatrix} , \quad \langle \hat{\Delta}^{L0} \rangle = v_L \begin{pmatrix} 1 \\ 0 \\ 0 \end{pmatrix} , \quad \langle \hat{\Delta}^{R0} \rangle = v_R \begin{pmatrix} 1 \\ \omega^2 \\ \omega \end{pmatrix} , \quad (\text{A.21})$$

$$\langle \eta^0 \rangle = u , \quad \langle \Delta_1^{L0} \rangle = \langle \Delta_2^{L0} \rangle = \langle \Delta_3^{L0} \rangle = u_L , \quad \langle \Delta_3^{R0} \rangle = u_R . \quad (\text{A.22})$$

where the $SU(2)_L$ nature of the fields is suppressed.

It can be seen from eq. (A.21) that the $A4$ triplet fields – $\hat{\Delta}^{L,R}$ and Φ – acquire vev which have been shown to be global minima in [22]. While this is certainly encouraging, that result is for one $A4$ triplet in isolation. Here there are many other fields and so it is not straight-forward to directly extend the results of [22].

In the following we list, sector by sector, the conditions under which the vev in eqs. (A.21) and (A.22) correspond to a minimum.

A.6.1 $SU(2)_L$ singlet sector:

The vev of the singlet fields $\hat{\Delta}_i^R$ and Δ_3^R are much larger than those of the $SU(2)_L$ doublet and triplet scalars. So, the contributions to the minimization equations from the inter-sector terms can be neglected.

Using the singlet sector potential in eq. (A.8) and the vev in eqs. (A.21) and (A.22) we get (bearing in mind v_R is real):

$$\frac{\partial V_{singlet}|_{min}}{\partial u_R^*} = 0 \Rightarrow u_R \left[m_{\Delta_3^R}^2 + \lambda_1^s u_R^* u_R + \frac{3}{2} \lambda_3^s v_R^2 \right] + 3v_R^2 [\lambda_4^s v_R + 2\lambda_5^s u_R^*] = 0 \quad , \quad (\text{A.23})$$

and

$$\begin{aligned} \frac{\partial V_{singlet}|_{min}}{\partial v_{Ri}^*} &= 0 \\ \Rightarrow v_R \left[m_{\Delta_R}^2 + 4\lambda_2^s v_R^2 + \frac{\lambda_3^s}{2} u_R^* u_R + \lambda_4^s v_R (2u_R + u_R^*) + 2\lambda_5^s u_R^2 \right] &= 0 \quad . \quad (\text{A.24}) \end{aligned}$$

A.6.2 $SU(2)_L$ doublet sector:

In this sector we have to include the contributions from both the doublet sector itself – eq. (A.11) – as well as the inter-sector terms in eq. (A.18). We define $V_{\mathcal{D}} = V_{doublet} + V_{sd}$.

In order that the potential minimum corresponds to the vev in eqs. (A.21) and (A.22) we must have:

$$\frac{\partial V_{\mathcal{D}}|_{min}}{\partial u^*} = 0 \Rightarrow u \left[2m_\eta^2 + 2\lambda_1^d u^* u + \lambda_3^d v^* v + \lambda_1^{sd} u_R^* u_R + 3\lambda_3^{sd} v_R^2 \right] = 0. \quad (\text{A.25})$$

and

$$\begin{aligned} \frac{\partial V_{\mathcal{D}}|_{min}}{\partial v_i^*} &= 0 \\ \Rightarrow \frac{v}{\sqrt{3}} \left[m_\Phi^2 + 4\lambda_2^d \left(\frac{v^* v}{3} \right) + \lambda_3^d u^* u + \frac{1}{2} \lambda_2^{sd} u_R^* u_R \right. \\ &\quad \left. + \lambda_4^{sd} (u_R^* + u_R) v_R + \frac{5}{4} \lambda_5^{sd} v_R^2 \right] = 0. \quad (\text{A.26}) \end{aligned}$$

Notice that one has to resort to some degree of fine-tuning to satisfy eqs. (A.25) and (A.26) which involve both $SU(2)_L$ doublet and singlet vev of quite different magnitudes.

A.6.3 $SU(2)_L$ triplet sector:

Using eqs. (A.8) and (A.20) we define $V_{\mathcal{T}} = V_{triplet} + V_{ts}$.

In this sector there are a plethora of couplings. To ease the presentation we choose

$$\begin{aligned} m_{\Delta_1^L} &= m_{\Delta_2^L} = m_{\Delta_3^L} = m_{\Delta^L} \quad ; \quad \lambda_{1_1}^t = \lambda_{1_2}^t = \lambda_{1_3}^t = \lambda_a^t \quad ; \quad \lambda_{4_1}^t = \lambda_{4_2}^t = \lambda_{4_3}^t = \lambda_b^t \\ \lambda_{22_1}^t &= \lambda_{23_2}^t = \lambda_{23_1}^t = \lambda_c^t \quad ; \quad \lambda_{8_1}^t = \lambda_{8_2}^t = \lambda_{8_3}^t = \lambda_d^t \quad ; \quad \lambda_{9_1}^t = \lambda_{9_2}^t = \lambda_{9_3}^t = \lambda_e^t \\ \lambda_{1_1}^{ts} &= \lambda_{1_2}^{ts} = \lambda_{1_3}^{ts} = \lambda_a^{ts} \quad ; \quad \lambda_{3_1}^{ts} = \lambda_{3_2}^{ts} = \lambda_{3_3}^{ts} = \lambda_b^{ts} \quad ; \quad \lambda_{5_1}^{ts} = \lambda_{5_2}^{ts} = \lambda_{5_3}^{ts} = \lambda_c^{ts} \\ \lambda_{1_0}^{ts} &= \lambda_{1_1}^{ts} = \lambda_{1_2}^{ts} = \lambda_d^{ts} \quad ; \quad \lambda_7^{ts} = \lambda_8^{ts} = \lambda_9^{ts} = \lambda_f^{ts}. \quad (\text{A.27}) \end{aligned}$$

For the minimization of $V_{\mathcal{F}}$ so as to arrive at the vev in eqs. (A.21) and (A.22) one must satisfy:

$$\begin{aligned}
\frac{\partial V_{\mathcal{F}}|_{min}}{\partial u_L^*} &= 0 \\
\Rightarrow u_L &\left[m_{\Delta L}^2 + (\lambda_a^t + \lambda_c^t) u_L^* u_L + \frac{1}{2} \lambda_b^t v_L^* v_L + \frac{1}{2} \lambda_a^{ts} u_R^* u_R + \frac{3}{2} \lambda_b^{ts} v_R^2 \right] \\
&+ 2v_L^2 u_L^* (\lambda_d^t + \lambda_e^t) + v_L v_R \left[-\frac{1}{2} \lambda_c^{ts} v_R + \lambda_d^{ts} u_R^* + \lambda_f^{ts} u_R \right] = 0.
\end{aligned} \tag{A.28}$$

Again:

$$\begin{aligned}
\frac{\partial V_{\mathcal{F}}|_{min}}{\partial v_{L1}^*} &= 0 \\
\Rightarrow v_L &\left[m_{\Delta L}^2 + \frac{3}{2} \lambda_b^t u_L^* u_L + 2\lambda_3^t v_L^* v_L + \frac{1}{2} \lambda_2^{ts} u_R^* u_R + \frac{3}{2} \lambda_4^{ts} v_R^2 \right] \\
&+ u_L \left[6u_L v_L^* (\lambda_d^t + \lambda_e^t) - \frac{3}{2} \lambda_c^{ts} v_R^2 + 3\lambda_f^{ts} u_R^* v_R + 3\lambda_d^{ts} u_R v_R \right] = 0.
\end{aligned} \tag{A.29}$$

Also we have

$$\begin{aligned}
\frac{\partial V_{\mathcal{F}}|_{min}}{\partial v_{L2}^*} &= \frac{\partial V_{\mathcal{F}}|_{min}}{\partial v_{L3}^*} = 0 \\
\Rightarrow v_L v_R &\left[-\frac{1}{4} \lambda_4^{ts} v_R + \lambda_6^{ts} (u_R^* + u_R) \right] = 0.
\end{aligned} \tag{A.30}$$

Here again fine-tuning is required to ensure that eqs. (A.28) - (A.30) are satisfied.

References

- [1] For the present status of θ_{13} see presentations from Double Chooz, RENO, Daya Bay, MINOS/MINOS+ and T2K at Neutrino 2014. <https://indico.fnal.gov/conferenceOtherViews.py?view=standard&confId=8022>.
- [2] B. Brahmachari and A. Raychaudhuri, Phys. Rev. D **86**, 051302 (2012) [arXiv:1204.5619 [hep-ph]]; S. Pramanick and A. Raychaudhuri, Phys. Rev. D **88**, 093009 (2013) [arXiv:1308.1445 [hep-ph]].
- [3] S. Pramanick and A. Raychaudhuri, Phys. Lett. B **746**, 237 (2015) [arXiv:1411.0320 [hep-ph]]; Int. J. Mod. Phys. A **30**, 1530036 (2015) [arXiv:1504.01555 [hep-ph]].
- [4] F. Vissani, JHEP **9811**, 025 (1998) [hep-ph/9810435]. Models with somewhat similar points of view as those espoused here are E. K. Akhmedov, Phys. Lett. B **467**, 95 (1999) [hep-ph/9909217] and M. Lindner and W. Rodejohann, JHEP **0705**, 089 (2007) [hep-ph/0703171].
- [5] For other recent work after the determination of θ_{13} see S. Antusch, S. F. King, C. Luhn and M. Spinrath, Nucl. Phys. B **856**, 328 (2012) [arXiv:1108.4278 [hep-ph]]; B. Adhikary, A. Ghosal and P. Roy, Int. J. Mod. Phys. A **28**, 1350118 (2013) arXiv:1210.5328 [hep-ph]; D. Aristizabal Sierra, I. de Medeiros Varzielas and E. Houet, Phys. Rev. D **87**, 093009 (2013) [arXiv:1302.6499]

- [hep-ph]]; R. Dutta, U. Ch, A. K. Giri and N. Sahu, *Int. J. Mod. Phys. A* **29**, 1450113 (2014) arXiv:1303.3357 [hep-ph]; L. J. Hall and G. G. Ross, *JHEP* **1311**, 091 (2013) arXiv:1303.6962 [hep-ph]; T. Araki, *PTEP* **2013**, 103B02 (2013) arXiv:1305.0248 [hep-ph]; A. E. Carcamo Hernandez, I. de Medeiros Varzielas, S. G. Kovalenko, H. Päs and I. Schmidt, *Phys. Rev. D* **88**, 076014 (2013) [arXiv:1307.6499 [hep-ph]]; M. -C. Chen, J. Huang, K. T. Mahanthappa and A. M. Wijangco, *JHEP* **1310**, 112 (2013) [arXiv:1307.7711] [hep-ph]; B. Brahmachari and P. Roy, *JHEP* **1502**, 135 (2015) [arXiv:1407.5293 [hep-ph]].
- [6] For a review see, for example, S. F. King and C. Luhn, *Rept. Prog. Phys.* **76**, 056201 (2013) [arXiv:1301.1340 [hep-ph]].
- [7] P. Minkowski, *Phys. Lett. B* **67**, 421 (1977); M. Gell-Mann, P. Ramond and R. Slansky, in *Supergravity*, p. 315, edited by F. van Nieuwenhuizen and D. Freedman, North Holland, Amsterdam, (1979); T. Yanagida, *Proc. of the Workshop on Unified Theory and the Baryon Number of the Universe*, KEK, Japan, (1979); S.L. Glashow, *NATO Sci. Ser. B* **59**, 687 (1980); R.N. Mohapatra and G. Senjanović, *Phys. Rev. D* **23**, 165 (1981).
- [8] E. Ma and G. Rajasekaran, *Phys. Rev. D* **64**, 113012 (2001) [hep-ph/0106291].
- [9] G. Altarelli and F. Feruglio, *Nucl. Phys. B* **741**, 215 (2006) [hep-ph/0512103]; H. Ishimori, T. Kobayashi, H. Ohki, Y. Shimizu, H. Okada and M. Tanimoto, *Prog. Theor. Phys. Suppl.* **183**, 1 (2010) [arXiv:1003.3552 [hep-th]].
- [10] For a sampling see, for example, F. Bazzocchi, S. Morisi and M. Picariello, *Phys. Lett. B* **659**, 628 (2008) [arXiv:0710.2928 [hep-ph]]; E. Ma, *Phys. Rev. D* **73**, 057304 (2006) [hep-ph/0511133]; P. Ciafaloni, M. Picariello, E. Torrente-Lujan and A. Urbano, *Phys. Rev. D* **79**, 116010 (2009) [arXiv:0901.2236 [hep-ph]].
- [11] E. Ma and D. Wegman, *Phys. Rev. Lett.* **107**, 061803 (2011) [arXiv:1106.4269 [hep-ph]]; S. Gupta, A. S. Joshipura and K. M. Patel, *Phys. Rev. D* **85**, 031903 (2012) [arXiv:1112.6113 [hep-ph]]; G. C. Branco, R. G. Felipe, F. R. Joaquim and H. Serodio, arXiv:1203.2646 [hep-ph]; B. Adhikary, B. Brahmachari, A. Ghosal, E. Ma and M. K. Parida, *Phys. Lett. B* **638**, 345 (2006) [hep-ph/0603059]; B. Karmakar and A. Sil, *Phys. Rev. D* **91**, 013004 (2015) [arXiv:1407.5826 [hep-ph]]; E. Ma, *Phys. Lett. B* **752**, 198 (2016) [arXiv:1510.02501 [hep-ph]].
- [12] S. K. Kang and M. Tanimoto, *Phys. Rev. D* **91**, no. 7, 073010 (2015) [arXiv:1501.07428 [hep-ph]].
- [13] J. Barry and W. Rodejohann, *Phys. Rev. D* **81**, 093002 (2010) [arXiv:1003.2385 [hep-ph]]; J. Barry, W. Rodejohann and H. Zhang, *JHEP* **1107**, 091 (2011) [arXiv:1105.3911 [hep-ph]]; A. Adulpravitchai and R. Takahashi, *JHEP* **1109**, 127 (2011) doi:10.1007/JHEP09(2011)127 [arXiv:1107.3829 [hep-ph]].
- [14] R. Gonzalez Felipe, H. Serodio and J. P. Silva, *Phys. Rev. D* **87**, 055010 (2013) [arXiv:1302.0861 [hep-ph]].
- [15] S. F. King and M. Malinsky, *Phys. Lett. B* **645**, 351 (2007) [hep-ph/0610250]; E. Ma, H. Sawanaka and M. Tanimoto, *Phys. Lett. B* **641**, 301 (2006) [hep-ph/0606103]; S. Morisi, M. Nebot, K. M. Patel, E. Peinado and J. W. F. Valle, *Phys. Rev. D* **88**, 036001 (2013) [arXiv:1303.4394 [hep-ph]]; S. Morisi, E. Peinado, Y. Shimizu and J. W. F. Valle, *Phys. Rev. D* **84**, 036003 (2011) [arXiv:1104.1633 [hep-ph]].

- [16] M. C. Gonzalez-Garcia, M. Maltoni, J. Salvado and T. Schwetz, *JHEP* **1212**, 123 (2012) [arXiv:1209.3023v3 [hep-ph]], NuFIT 1.3 (2014).
- [17] D. V. Forero, M. Tortola and J. W. F. Valle, *Phys. Rev. D* **86**, 073012 (2012) [arXiv:1205.4018 [hep-ph]].
- [18] C. Bronner on behalf of the T2K collaboration, Talk at the International Conference on Massive Neutrinos, Nanyang Technological University, Singapore, February 2015.
- [19] M. Haag [KATRIN Collaboration], *PoS EPS -HEP2013*, 518 (2013).
- [20] Ryan Patterson [for the NO ν A Collaboration], Joint Experimental and Theoretical Seminar, Fermilab, August 06, 2015.
- [21] See, for example, G. Drexlin, V. Hannen, S. Mertens and C. Weinheimer, *Adv. High Energy Phys.* **2013**, 293986 (2013) [arXiv:1307.0101 [physics.ins-det]].
- [22] A. Degee, I. P. Ivanov and V. Keus, *JHEP* **1302**, 125 (2013) [arXiv:1211.4989 [hep-ph]].
- [23] R. Gonzalez Felipe, H. Serodio and J. P. Silva, *Phys. Rev. D* **88**, 015015 (2013) [arXiv:1304.3468 [hep-ph]].